Research Papers
Issue 2011/12
November 2012

Impacts on Soil and Coast (ISC) Division

Implementation of a numerical scheme based on the Dual Time Stepping in COSMO LM: idealized test cases

By **dr. Giovanni Petrone**
Impacts on Soil and Coast Division (ISC), CMCC
giovanni.petrone@cmcc.it

SUMMARY This paper is part of research on the development and testing of a modified version of COSMO LM, that is aimed to assess the feasibility of a time integration technique called Dual Time Stepping (DTS). In a previous paper it was described the implemention of the proposed time integration core with an application for a steady mountain ideal flow. In the present work the DTS scheme has been applied to an unsteady idealized test case, the nonhydrostatic inertia-gravity wave, that involves the evolution of a potential temperature perturbation in a channel. This study on idealized cases will be followed, in future research, by an assessment of the proposed numerical scheme on a realistic test case for Meteorology and Climatology.

The work here presented is carried out under the technical supervision of ing. Pier Luigi Vitagliano (CIRA).

INTRODUCTION AND MOTIVATIONS

As stated in a previous research paper [1], no evidence of a previous attempt to use Dual Time Stepping (DTS) in Numerical Weather Prediction (WPN) has been found in literature by the author. In order to reduce the complexity of the re-coding effort, the original framework of COSMO [2] has been used with a limited amount of modifications. The aim of the present work is to assess the use of the DTS scheme on an idealized test case, extensively studied in the reference literature [3, 4], by comparing the results obtained with the original version of COSMO. Therefore the non hydrostatic inertia-gravity wave test is particularly interesting since it allows to compare the evolution of a gravity wave without any disturbance introduced by the parametrizations and/or the orography. The original version of COSMO adopts the time-splitting scheme of Wicker and Skamarock [6] , where the slow processes are integrated with a second-order three-stage RK scheme and the fast ones with a forward-backward scheme in the horizontal direction and an implicit Crank- Nicholson scheme in vertical. In the DTS version of COSMO all (fast and slow) processes are treated using the same scheme.

INERTIA-GRAVITY WAVES

The first test case that we use was proposed by Skamarock et al. [3]. The nonhydrostatic inertia-gravity wave involves the evolution of a potential temperature perturbation in a channel with a background flow. A lot of meteorological models, like COSMO, discretise and integrate the advection and the fast modes (sound, gravity waves) differently. The introduction of a background flow serves as a test for a good coupling of these processes. The initial conditions we use are identical to those of Giraldo [4]. The initial state of the atmosphere is taken to have a constant mean flow in a uniformly stratified atmosphere with a constant Brunt- $V\ddot{a}is\ddot{a}l\ddot{a}$ frequency. Skamarock and Klemp gave an analytic solution for this test but, unfortunately, it is only valid for the Boussinesq equations. Therefore we compare only the maximum and minimum values of potential temperature perturbartion and vertical velocity perturbation with those reported by Giraldo. Different settings of COSMO were examined.

The second test case that we use is based on the work of Baldauf [5], where a slightly modified version of the idealised test setup used by Skamarock and Klemp is proposed: the modification allows to derive an exact analytical solution for the compressible, non-hydrostatic Euler equations, for the quasi linear 2-dimensional expansion of sound and gravity waves in a channel induced by a weak warm bubble.

We introduce here some general remarks about the numerical simulation. Every physical parameterisation in the numerical model must be switched off, in particular (turbulent) diffusion and boundary layer treatment. Furthermore, free slip boundary conditions must be prescribed at the top and the bottom of the domain . Damping layers at the lateral boundaries and Rayleigh damping must be switched off, too. To be in a strongly dominated linear regime, the initial temperature perturbation must be relatively small (0.01 K). Consequently, only small pressure perturbations are produced which must be compared with the total pressure $\mathcal{O}(10^5$ Pa). Thus double precision for all floating point operations is recommended.

INERTIA-GRAVITY WAVES IN THE ORIGINAL COSMO

In the first test case the initial state of the atmosphere is taken to have a constant horizontal mean flow of $u = 20m/s$ in a uniformly stratified atmosphere with a $Brunt - Väisälä$ frequency of $\mathcal{N} = 0.01/s$. The domain is defined as $(x, z) \in [0, 300000]m \times [0, 10000]m$ with $t \in [0, 3000]s$. Figure 1 shows the iso-contours of potential temperature pertubation at the beginning of the simulation, where a hot bubble ($\Delta\Theta$=0.01^{o}C) is placed at x = 100000 m, following the same perturbation law used by Giraldo.

No-flux boundary conditions are used along the bottom and top boundaries, that are modeled as a rigid-lid-free-slip. A the lateral boundaries inflow/outflow free-slip conditions are imposed. The results are considered after 3000 s of simulation, when the initial disturbance has been propagated. A first study has been carried out on the original version of COSMO in order to assess the grid convergence and analyze the sensitivity of the solution to the numerical parameters used in the time integration scheme. More in detail, it has been assessed the impact of the weigthing applied to the numerical time derivative in the fast waves implicit scheme. Further studies have been carried out using different advection orders, but no significant changes have been noticed and the results have been not reported. A complete summary of the results can be found in Tables 1 and 2. The solution corresponding to the case labeled as $\mathbf{OR}\beta\mathbf{9}$ has been reported in the following figures.

The iso-contours of potential temperature pertubation ($\Delta\Theta$) after 3000 s of simulation are reported in Figure 2 , showing the simmetry of the waves about the position x = 160000 m.

The simmetry can be either observed in Figure 3, where the iso-contours of the vertical velocity (w) have been reported. We use the same contouring interval used in Giraldo and our results look quite similar.

Figure 4 shows the iso-contours of horizontal velocity perturbation (δu) after 3000 s of simulation, using the original routines of COSMO: it is possible to notice the simmetrical behaviour of the inertia-gravity waves.

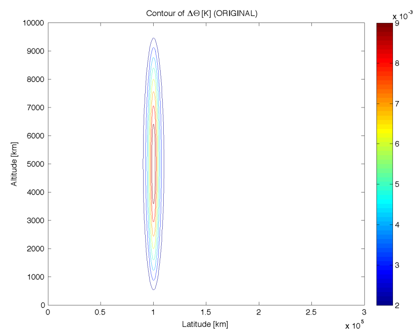

Figure 1:
Contour of $\delta\Theta$, dt=12 s, t=0 s

Source: Original COSMO

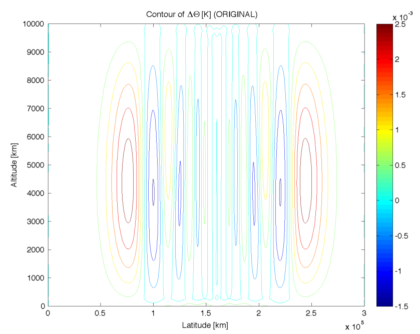

Figure 2:
Contour of $\delta\Theta$, dt=12 s, t=3000 s

Source: Original COSMO

The distribution of the potential temperature pertubation ($\Delta\Theta$) has been reported at an altitude of z=5000 m in Figure 5 . It is interesting to notice the particular behaviour of the potential temperature pertubation around the position x = 160000 m, where a certain time resolution is required to obtain this two-small-peaks structure. This aspect will be analyzed in the following sections where the dependency of the solution on the time resolution will be assessed.

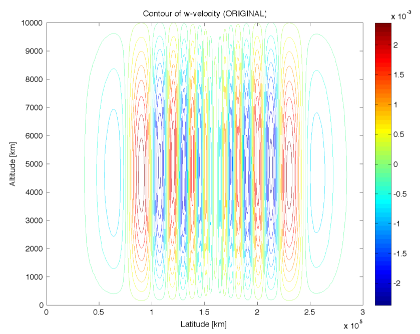

Figure 3:
Contour of w-velocity, dt=12 s, t=3000 s

Source: Original COSMO

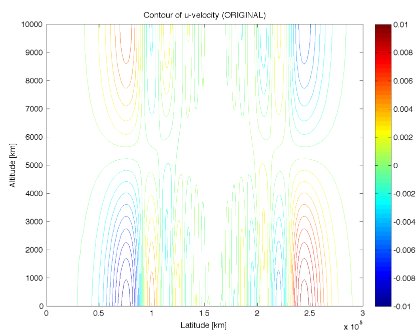

Figure 4:
Contour of δu-velocity, dt=12 s, t=3000 s

Source: Original COSMO

GRID CONVERGENCE STUDY

In this section we analyze the impact of the spatial resolution (Δx and Δz) and time resolution (dt) on the results obtained with the original routines of COSMO. Several simulations were carried out to assess the grid convergence on the maximum potential temperature perturbation (max $\Delta\Theta$), the minimum potential temperature perturbation (min $\Delta\Theta$), the maximum vertical velocity (max w) and the minimum vertical velocity (min w) after 3000s of simulation, as reported in Table 1. The reference results are those reported by Giraldo, with a horizontal and vertical resolution of 0.25 km and a time step of 12 s.

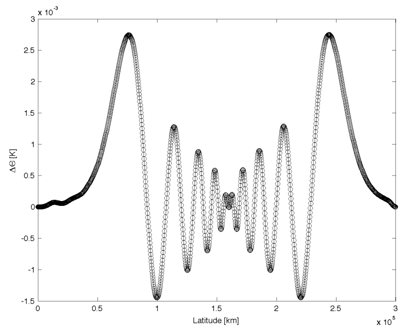

Figure 5:
Distribution of $\delta\Theta$ at the heigth of 5000 m, dt=12 s, t=3000 s

Source: Original COSMO

The cases labeled as **OR2**, **OR5**, **OR6**, **OR7** and **OR8** show the dependency of the solution on the time step, with dt ranging from 3 s to 50 s, with a constant horizontal resolution of Δx=1 km and Δz=0.5 km. The comparison among the cases labeled ad **OR1**, **OR2**, **OR3** and **OR4** show the dependency of the solution on the vertical resolution with Δz ranging from 1 km to 0.125 km and a constant Δx=1 km, dt=12 s . Furthermore the dependecy on the horizontal resolution can be assessed by comparing the cases labeled as **OR1**, **OR9**, **OR10** and **OR3**, **OR13**. The potential temperature perturbation ($\Delta\Theta$) converges toward the results obtained by Giraldo as the resolution increases, while the vertical velocity perturbation remains different even for the finest resolution. The results show that the depedency of the solution on the horizontal and vertical resolution becomes negligible with a grid spacing smaller than 0.25 km, while the dependency on the time step seems more tricky. Two effects have to be considered. At first, the fast (sound and gravity) waves in COSMO are integrated with a smaller and roughly constant time step, evaluated independently on the input (longer) time step. Moreover the fast waves time derivative depends on the weighting parameters adopted in the implicit formulation.

Finally it has been noticed that the grid convergence to the solution obtained by Giraldo is almost of second order for the potential temperature perturbation, while the vertical velocity perturbation does not show the same behaviour. In order to produce a more consistent comparison of the results with the ones obtained by Giraldo, the case labeled as **OR13** has been chosen to perform a further sensitivity study on the values used for time-weighting in the treatment of acoustic (sound) waves and gravity waves.

SENSITIVITY ON THE TIME-WEIGHTING PARAMETERS

In this section we analyze the impact of the time weighting parameters of COSMO on the results obtained with the original routines of COSMO. We recall here that βsw is the value of the β-parameter used for time-weighting of the future values in the vertically implicit treatment of acoustic (sound) waves. Indeed βsw=0 gives a time-centred average with no damping, βsw=1 results in a fully implicit vertical scheme with strong damping of acoustic and gravity wave modes. The parameter βgw is the same as βsw, but used for gravity waves. Both these parameters act on the w-velocity equation. On the other hand we have the parameter $\beta 2sw$, same as βsw but used in the p*, T* dynamics for sound waves, and the parameter $\beta 2gw$, same as βgw but used in the p*, T* dynamics for gravity waves. Since slight positive off-centering is recommended to damp disturbances, COSMO uses a default value of 0.4 for all these parameters. We noticed that the values of (βsw/$\beta 2sw$/βgw/$\beta 2gw$) highly impact the simmetry and amplitude of the waves in the solution obtained after 3000s of simulation. Therefore we performed the sensitivity study reported in Table 2. Figure 6 shows the iso-contours of horizontal velocity perturbation (δu) after 3000s of simulation for the case labeled as **ORβ2** . It's possible to notice that using (βsw/$\beta 2sw$/βgw/$\beta 2gw$) =(0/0/0/0) results in a presence of high-frequency noise in the horizontal velocity distrubution.

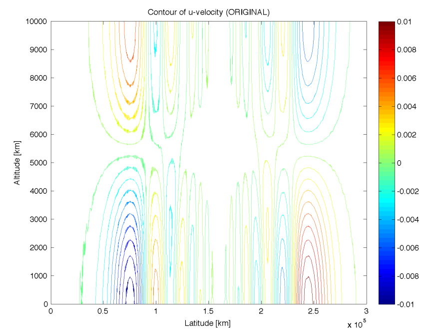

Figure 6:
Contour of δu-velocity, dt=12 s, t=3000 s.
(βsw/$\beta 2sw$/βgw/$\beta 2gw$)=(0/0/0/0)

Source: Original COSMO

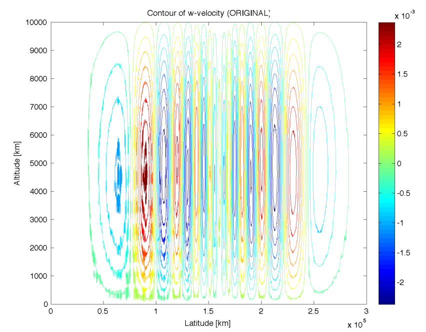

Figure 7:
Contour of w-velocity, dt=12 s, t=3000 s.
(βsw/$\beta 2sw$/βgw/$\beta 2gw$)=(0/0/0/0)

Source: Original COSMO

This effect is highlithed in the distribution of the w-velocity, reported in Figure 7. At least a non-zero value of one element among ($\beta sw/\beta 2sw/\beta gw/\beta 2gw$) is required to damp these oscillations, while better results and simmetrical behaviour can be achieved reducing them with respect to the default settings.

In order to obtain a better agreement with the results by Giraldo, the case labeled as $\mathbf{OR}\beta\mathbf{9}$, where only $\beta 2sw$=0.4, has been chosen in order to compare the original routines of COSMO with the DTS modifications introduced in this paper.

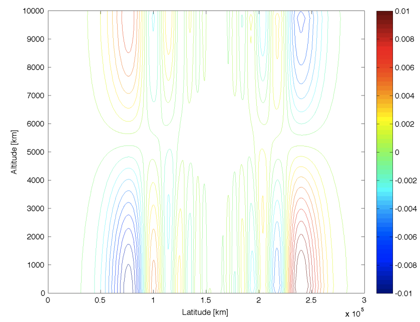

Figure 8:
Contour of δ u-velocity, dt=3 s, t=3000 s

Source: DTS COSMO

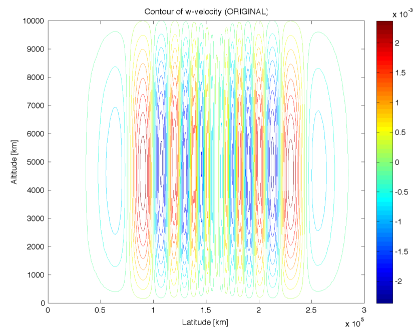

Figure 9:
Contour of w-velocity, dt=3 s, t=3000 s

Source: DTS COSMO

INERTIA-GRAVITY WAVES IN THE DTS COSMO

Figure 8 shows the iso-contours of horizontal velocity perturbation (δu) after 3000 s of simulation, using the modified DTS routines of COSMO: it is possible to notice that the structure of the u-velocity field corresponds to the one obtained with the original routines, in Figure 4 . For a sake of clarity the same contour intervals have been used. Comparing the w-velocity fields, i.e. Figure 9 and Figure 3, and the potential temperature perturbation fields, i.e. Figure 10 and Figure 2, it is possible to notice that the DTS predictions using a phisical time step of dt=3 s give results that are consinstent with the ones obtained in the case labeled as $\mathbf{OR}\beta\mathbf{9}$ in the original COSMO.

DUAL TIME RESOLUTION CONVERGENCE STUDY

The time-splitting formulation implemented in the original COSMO takes advantage of a time accuracy in the resolution of the fast processes given by the use of small time steps. Since we're considering a gravity (fast) waves test case, each physical time step in DTS COSMO has to be small enough to ensure a good resolution of the fast processes involved in the governing equations. In order to assess the minimum requirements for DTS COSMO, time convergence study has been carried out and the results collected in Table 3. For a better understanding of the impact of the dual time resolution in comparison with the reference case ($\mathbf{OR}\beta\mathbf{9}$), the distribution of the potential temperature pertubation ($\Delta\Theta$) has been reported at an altitude of z=5000m in Figure 11 . Comparing the cases labeled as $\mathbf{DTS1}$(dt=12 s), $\mathbf{DTS2}$(dt=6 s) and $\mathbf{DTS3}$(dt=3 s), it is possible to notice that a time step of dt=3 s is required to obtain a good agreement of the potential temperature pertubation with the reference case. A detail of the potential temperature pertubation at an heigth of 5000 m among the latitudes of x=155000 m

Table 1
Grid convegence: inertia-gravity waves

CASE	Δx [km]	Δz [km]	dt [s]	max $\Delta\Theta$ [K]	min $\Delta\Theta$ [K]	max w [m/s]	min w [m/s]
Giraldo	0,25	0,25	12	0,002787	-0,001518	0,002698	-0,002774
OR1	1	1	12	0,002752	-0,001472	0,002575	-0,002369
OR2	1	0,5	12	0,002781	-0,001498	0,002611	-0,002374
OR3	1	0,25	12	0,002786	-0,001503	0,002610	-0,002378
OR4	1	0,125	12	0,002786	-0,001504	0,002609	-0,002378
OR5	1	0,5	3	0,002781	-0,001492	0,002607	-0,002360
OR6	1	0,5	6	0,002781	-0,001497	0,002611	-0,002371
OR7	1	0,5	24	0,002785	-0,001499	0,002612	-0,002375
OR8	1	0,5	50	0,002908	-0,001532	0,002700	-0,002400
OR9	2	1	12	0,002734	-0,001431	0,002520	-0,002235
OR10	4	1	12	0,002607	-0,001018	0,002147	-0,001174
OR11	0,125	0,25	3	0,002794	-0,001517	0,002631	-0,002439
OR12	0,125	0,25	6	0,002794	-0,001517	0,002610	-0,002441
OR13	0,25	0,25	12	0,002794	-0,001515	0,002616	-0,002406

Table 2
Sensitivity of case OR13 on βs: inertia-gravity waves

CASE	max $\Delta\Theta$ [K]	min $\Delta\Theta$ [K]	min w [m/s]	max w [m/s]	βsw	$\beta 2sw$	βgw	$\beta 2gw$
Giraldo	0,002787	-0,001518	0,002698	-0,002774				
ORβ1	0,002794	-0,001515	0,002616	-0,002406	0,4	0,4	0,4	0,4
ORβ2	0,002794	-0,001515	0,002528	-0,002660	0,0	0,0	0,0	0,0
ORβ3	0,002803	-0,001526	0,002619	-0,002442	0,4	0,4	0,0	0,0
ORβ4	0,002799	-0,001518	0,002619	-0,002423	0,4	0,4	0,4	0,0
ORβ5	0,002796	-0,001516	0,002617	-0,002408	0,4	0,4	0,0	0,4
ORβ6	0,002789	-0,001511	0,002532	-0,002575	0,0	0,0	0,4	0,4
ORβ7	0,002792	-0,001514	0,002580	-0,002432	0,0	0,4	0,4	0,4
ORβ8	0,002792	-0,001514	0,002580	-0,002432	0,4	0,0	0,4	0,4
ORβ9	0,002799	-0,001519	0,002578	-0,002475	0,0	0,4	0,0	0,0
ORβ10	0,002799	-0,001520	0,002578	-0,002475	0,4	0,0	0,0	0,0
ORβ11	0,002793	-0,001515	0,002524	-0,002652	0,0	0,1	0,0	0,0
ORβ12	0,002795	-0,001517	0,002480	-0,002577	0,1	0,0	0,0	0,0

Table 3
Time resolution in DTS: inertia-gravity waves

CA SE	Δx [km]	Δz [km]	dt [s]	max $\Delta\Theta$ [K]	min $\Delta\Theta$ [K]	min w [m/s]	max w [m/s]
Giraldo	0,25	0,25	12	0,002787	-0,001518	0,002698	-0,002774
DTS1	0,25	0,25	12	0.002839	-0.001468	0.002635	-0.002360
DTS2	0,25	0,25	6	0.002847	-0.001449	0.002613	-0.002381
DTS3	0,25	0,25	3	0.0028165	-0.001498	0.002605	-0.002404

and x=165000 m has been reported in Figure 16. A dual time step of dt=12 s is not enough to capture the two peaks of potential temperature pertubation, while the results get closer to the

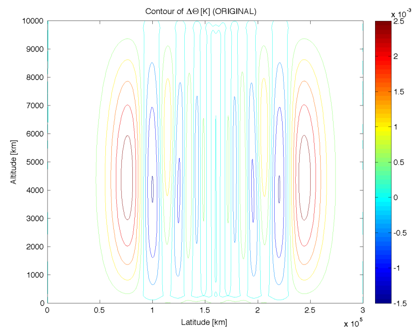

Figure 10:
Contour of $\delta\Theta$, dt=3 s, t=3000 s

Source: DTS COSMO

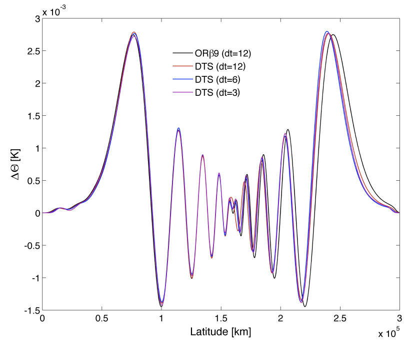

Figure 11:
Distribution of $\delta\Theta$ at the heigth of 5000 m using differents dual time resolutions

Source: DTS COSMO

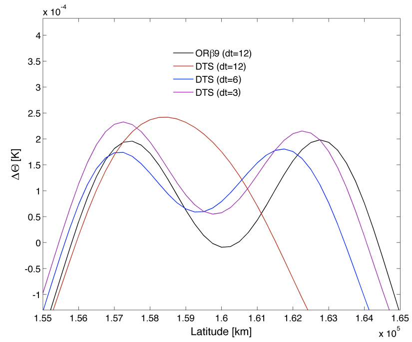

Figure 12:
Distribution of $\delta\Theta$ at the heigth of 5000 m using differents dual time resolutions - detail

Source: DTS COSMO

original COSMO as the time step decreases.

The threshold chosen for the convergence of the dual time iterations is the decay of 2.5 (logaritmic) levels in the w-component velocity residual.

ANALYTICAL SOLUTION FOR THE LINEAR GRAVITY WAVES

In the second test case we consider the evolution of a small initial deviation from a stratified atmosphere which is contained in a two-dimensional channel. The stratified atmosphere is isothermal with the absolute temperature T_0, which leads to a constant $Brunt - Väisälä$ frequency and a constant sound speed. Under this assumption an analytical solution can be derived for linear gravity waves by means of a Bretherton[10] transformation, as shown by Baldauf [9]. At the top and the bottom free slip boundary conditions are used. At the lateral boundaries periodic boundary conditions are used. The equations and the boundary conditions are satisfied for a stationary, hydrostatic, horizontally homogeneous, and isothermal background state. The warm bubble is initialised by the following deviations from the background atmosphere:

$$\begin{aligned} T'(r,t=0) &= e^{+\frac{1}{2}\delta z} \cdot T_b(r,t=0) \\ p'(r,t=0) &= 0 \\ \rho'(r,t=0) &= e^{-\frac{1}{2}\delta z} \cdot \rho_b(r,t=0) \end{aligned} \tag{1}$$

with the Bretherton-transformed temperature deviation

$$T_b(r,t=0) = \Delta T \cdot e^{-\frac{(x-x_c)^2}{d^2}} \cdot sin\pi\frac{z}{H} \tag{2}$$

where ΔT is the temperature perturbartion, x_c is the initial position of the warm bubble, d the radius of the bubble, H the heigth of the channel and $\delta = \frac{g}{RT_0}$ the Bretherton-height parameter. The appropriate density deviation can be computed from the linearised ideal gas law. A Gaussian shape of the bubble in horizontal direction has been implemented in COSMO, as shown in [5].

ANALYTICAL SOLUTION VS ORIGINAL COSMO SOLUTION

In the following we report the comparison between the potential temperature perturbation ($\Delta\Theta$) and the w-velocity perturbation (Δw), after 1800s, using four different grid resolutions (see Table 4) in the original COSMO. The test case was carried out with the following parameters for the warm bubble: ΔT=0.01 K, the radius d=5000 m, and the initial position x_c = 100 km. The domain is defined as $(x, z) \in [0, 300000]m \times [0, 10000]m$ with $t \in [0, 1800]s$. For the background atmosphere, we take T_0 = 250 K and p_{sl} = 10^5 Pa at sea level. In addition, we use the following constants for the dry air R = 287.05 J/kg/K, c_p = 1005.0 J/kg/K, $c_v = c_p - R$, and the gravity acceleration as g = 9.80665 m/s^2. We prescribe a constant background flow of u_0 = 20 m/s. A constant vertical resolution of the grid of Δz =125 m has been fixed. The weighting parameters of the time-derivative (βsw/$\beta 2sw$/βgw) have been set equal to zero, while $\beta 2gw$ equals 0.1 to avoid numerical high-frequency oscillations of the results. A small modification has been introduced in COSMO to reduce the small time step of the fast waves by five times with respect to its standard value, in order to obtain an enhanced time resolution of the gravity waves. Figures 15,16,17 and 18 show the convegence of the potential temperature perturbation and the w-velocity perturbation to the analytical solution at an heigth of 5000 m. As proposed in [5], to quantify the error of a solution Ψ of COSMO, we use the mean value of the error in a suitable norm:

$$L^2(\Psi) = \left(\frac{1}{N_x N_z}\sum_{i=1}^{N_x}\sum_{k=1}^{N_z}|\Psi - \Psi_{ref}|^2\right)^{\frac{1}{2}} \tag{3}$$

$$L^\infty(\Psi) = \max|\Psi - \Psi_{ref}|$$

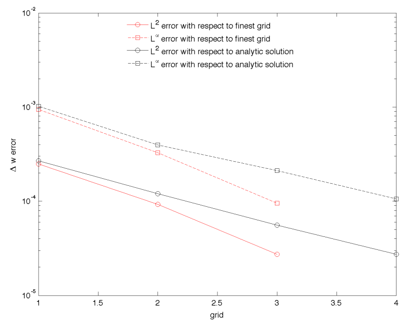

Figure 13:
L^2-norm and L^∞-norm of the w-velocity perturbation: numerical and analytic convergence.

Source: original COSMO

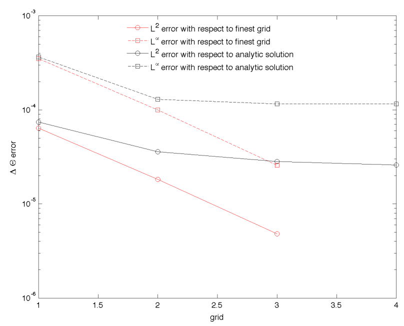

Figure 14:
L^2-norm and L^∞-norm of the potential temperature perturbation: numerical and analytic convergence.

Source: original COSMO

The grid convergence using the L^2-norm and L^∞-norm of the potential temperature perturbation and the w-velocity perturbation have been reported in Figures 13 and 14, using respectively the finest grid and the analytical solution as reference.

Table 4
Analytic grid convergence in original COSMO: inertia-gravity waves

GRID	Δx [m]	dt [s]	L^{∞} error on $\Delta\Theta$	L_2 error on $\Delta\Theta$	L^{∞} error on Δ w	L_2 error on Δ w
1	1000	20.0	$0.3661{\cdot}10^{-3}$	$0.7430{\cdot}10^{-4}$	$0.1022{\cdot}10^{-2}$	$0.2691{\cdot}10^{-3}$
2	500	10.0	$0.1299{\cdot}10^{-3}$	$0.3586{\cdot}10^{-4}$	$0.0396{\cdot}10^{-2}$	$0.1201{\cdot}10^{-3}$
3	250	5.0	$0.1159{\cdot}10^{-3}$	$0.2819{\cdot}10^{-4}$	$0.0211{\cdot}10^{-2}$	$0.0559{\cdot}10^{-3}$
4	125	2.5	$0.1157{\cdot}10^{-3}$	$0.2596{\cdot}10^{-4}$	$0.0106{\cdot}10^{-2}$	$0.0273{\cdot}10^{-3}$

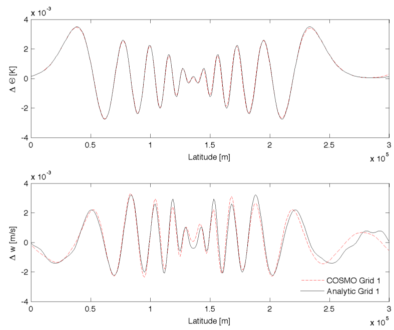

Figure 15:
potential temperature perturbation ($\Delta\Theta$ [K]) and w-velocity perturbation (Δw) after 1800 s: grid 1 vs Analytic solution. ($\beta sw/\beta 2sw/\beta gw/\beta 2gw$)=(0/0/0/0.1) and reduced small time step.

Source: original COSMO

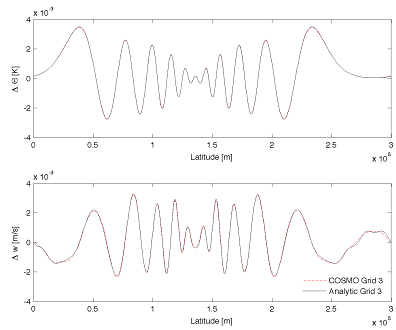

Figure 17:
potential temperature perturbation ($\Delta\Theta$ [K]) and w-velocity perturbation (Δw) after 1800 s: grid 3 vs Analytic solution.($\beta sw/\beta 2sw/\beta gw/\beta 2gw$)=(0/0/0/0.1 and reduced small time step.

Source: original COSMO

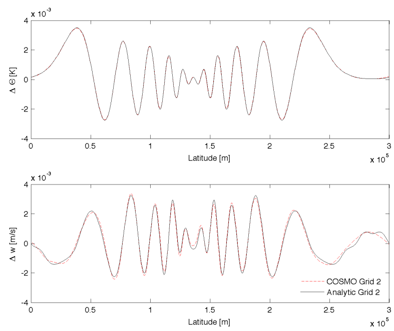

Figure 16:
potential temperature perturbation ($\Delta\Theta$ [K]) and w-velocity perturbation (Δw) after 1800 s: grid 2 vs Analytic solution. ($\beta sw/\beta 2sw/\beta gw/\beta 2gw$)=(0/0/0/0.1 and reduced small time step.

Source: original COSMO

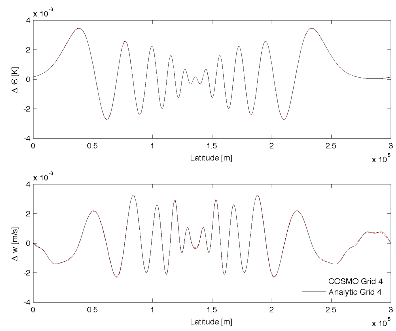

Figure 18:
potential temperature perturbation ($\Delta\Theta$ [K]) and w-velocity perturbation (Δw) after 1800 s: grid 4 vs Analytic solution. ($\beta sw/\beta 2sw/\beta gw/\beta 2gw$)=(0/0/0/0.1) and reduced small time step.

Source: original COSMO

The importance of considering a variation of the weighting parameters with respect to the default values of 0.4 is shown comparing the Figure 18 and Figure 19, obtained for the finest grid.

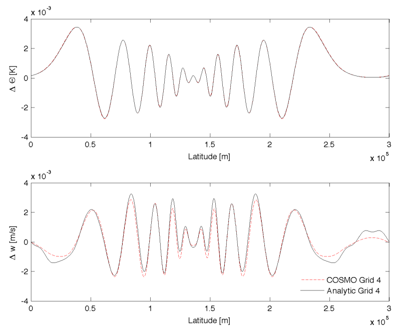

Figure 19:
potential temperature perturbation ($\Delta\Theta$ [K]) and w-velocity perturbation (Δw) after 1800 s: grid 4 vs Analytic solution. ($\beta sw/\beta 2sw/\beta gw/\beta 2gw$) = (0.4/0.4/0.4/0.4) and original small time step.

Source: original COSMO

The importance of considering a reduction of the small time step used in the fast processes with respect to the value computed by COSMO is shown comparing the Figure 18 and Figure 20, obtained for the finest grid.

ANALYTICAL SOLUTION VS DTS COSMO SOLUTION

In the following we report the comparison between the potential temperature perturbation ($\Delta\Theta$) and the w-velocity perturbation (Δw), after 1800 s, using three different grid resolutions (see Table 5) in the DTS COSMO.

When not explicitely specified, the previous settings used in the orginal COSMO have been kept. The convergence threshold in DTS COSMO has been set to a decay of three logaritimic levels in the residual of the pressure perturbation. The time step used in DTS COSMO equals to dt=0.36 s, the same time

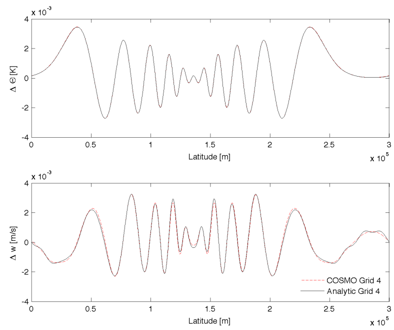

Figure 20:
potential temperature perturbation ($\Delta\Theta$ [K]) and w-velocity perturbation (Δw) after 1800 s: grid 4 vs Analytic solution. ($\beta sw/\beta 2sw/\beta gw/\beta 2gw$) = (0/0/0/0.1) and original small time step.

Source: original COSMO

step used in the original COSMO to handle the fast processes in the governing equation. Figures 23,24 and 25 show the convegence of the potential temperature perturbation and the w-velocity perturbation to the analytical solution at an heigth of 5000 m.

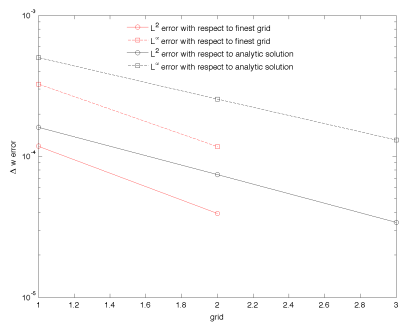

Figure 21:
L^2-norm and L^∞-norm of the w-velocity perturbation: numerical and analytic convergence.

Source: DTS COSMO

The grid convergence using the L^2-norm and L^∞-norm of the potential temperature perturbation and the w-velocity perturbation have been reported in Figures 21 and 22, using respec-

Table 5
Analytic grid convergence in DTS COSMO: inertia-gravity waves

GRID	Δx [m]	dt [s]	L^∞ error on $\Delta\Theta$	L_2 error on $\Delta\Theta$	L^∞ error on Δ w	L_2 error on Δ w
1	1000	0.36	$2.1610\cdot10^{-3}$	$5.4994\cdot10^{-4}$	$5.0314\cdot10^{-4}$	$1.6081\cdot10^{-4}$
2	500	0.36	$1.1589\cdot10^{-3}$	$3.1232\cdot10^{-4}$	$2.5446\cdot10^{-4}$	$7.4338\cdot10^{-5}$
3	250	0.36	$1.1603\cdot10^{-3}$	$2.7182\cdot10^{-4}$	$1.3052\cdot10^{-4}$	$3.4066\cdot10^{-5}$

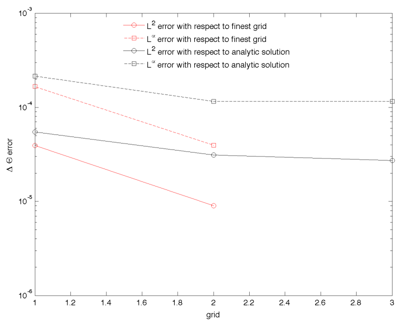

Figure 22:
L^2-norm and L^∞-norm of the potential temperature perturbation: numerical and analytic convergence.

Source: DTS COSMO

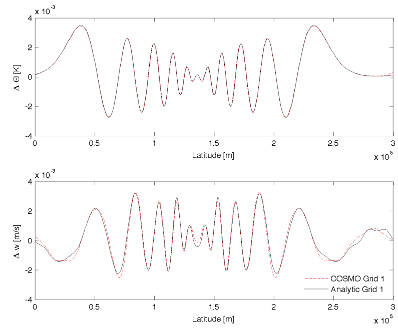

Figure 23:
potential temperature perturbation ($\Delta\Theta$ [K]) and w-velocity perturbation (Δw) after 1800 s: grid 1 vs Analytic solution. Threshold of 3 logaritmic levels in the pressure perturbation residual decay.

Source: DTS COSMO

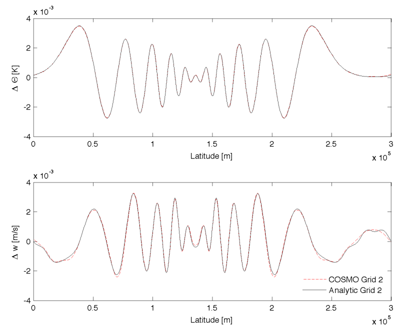

Figure 24:
potential temperature perturbation ($\Delta\Theta$ [K]) and w-velocity perturbation (Δw) after 1800 s: grid 2 vs Analytic solution. Threshold of 3 logaritmic levels in the pressure perturbation residual decay

Source: DTS COSMO

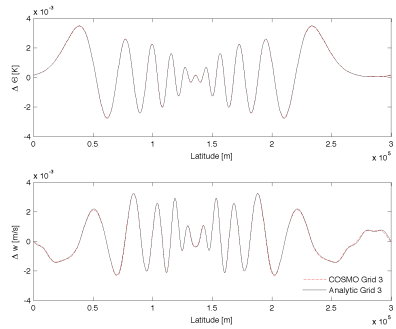

Figure 25:
potential temperature perturbation ($\Delta\Theta$ [K]) and w-velocity perturbation (Δw) after 1800 s: grid 3 vs Analytic solution. Threshold of 3 logaritmic levels in the pressure perturbation residual decay.

Source: DTS COSMO

tively the finest grid and the analytical solution as reference. Comparing Table 4 and Table 5, it's possible to notice that using the same time resolution in the fast and slow processes lead to a better agreement with analytic results, even when using the coarsest grid. To conclude this paper we report in Figure 26 the solution obtained on the coarsest grid using a decay of two logaritmic levels in the residual of the pressure perturbaton. Comparing the results with those obtained in Figure 23, it is possible to notice the importance of ensuring a certain accuracy in the prediction of the pressure perturbation to obtain a better comparison with the analytic results. The author reccomends at most three logaritmic decay in the pressure perturbation residual since additional studies, not reported in this paper, have shown no significant improvement in the quality of the results when further increasing this treshold. The pressure perturbation residual has been adopted to control the DTS convergence since it's the slowest converging one due to preconditioning.

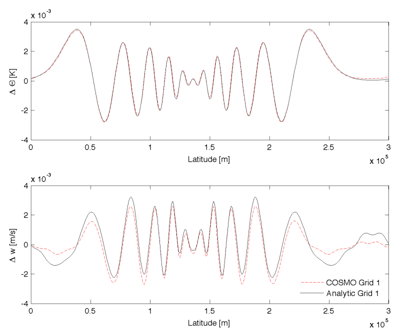

Figure 26:
potential temperature perturbation ($\Delta\Theta$ [K]) and w-velocity perturbation (Δw) after 1800 s: grid 1 vs Analytic solution. Threshold of 2 logaritmic levels in the pressure perturbation residual decay.

Source: DTS COSMO

CONCLUSIONS

In this paper the numerical perfomances of the DTS have been assessed in comparison with the operational COSMO model Runge Kutta scheme on an ideal test case. The inertia-gravity waves case shows that the DTS integration is able to give comparable results to the existing COSMO, both in terms of accuracy and mesh convergence, leading the author to further investigate the advantages and disadvantages of the proposed methodology with a real test case in Metereology and Climatology.

ACKNOWLEDGMENTS

The author gratefully acknowledges the support of Michael Baldauf, who provided the mathematical and numerical instruments to reproduce the exact analytical solution for the compressible, non-hydrostatic Euler equations, for the quasi linear 2-dimensional expansion of sound and gravity waves in a channel induced by a weak warm bubble .

Bibliography

[1] Petrone, G., Theoretical study and software design for the implementation of a numerical scheme based on the Dual Time Stepping in COSMO LM, CMCC Research Papers Issue RP0135

[2] Schattler, U., Doms, G., and Schraff., C., Nonhydrostatic Regional COSMO-Model. Part VII: User's Guide, COSMO-Model 4.21, www.cosmo-model, December 2011

[3] Skamarock WC, Klemp JB. 1994. Efficiency and accuracy of the Klemp-Wilhelmson Time-Splitting scheme. Mon. Wea. Rev. 122: 2623-2630.

[4] Giraldo, F.X., Restelli, M., A study of spectral element and discontinuous Galerkin methods for the Navier-Stokes equations in nonhydrostatic mesoscale atmospheric modeling: Equation sets and test cases. Journal of Computational Physics vol. 227 issue 8 April 1, 2008. p. 3849-3877.

[5] Baldauf, M. 2008. A linear solution for flow over mountains and its comparison with the COSMO model. COSMO-Newsletter 9: 19-24.

[6] Wicker, L. J., Skamarock, W. C., Time-splitting methods for elastic models using forward time schemes, Mon. Wea. Rev., 130, 2088-2097, 2002

[7] Marchuk, J., Numerical Methods in Weather Forecasting (in Russian), Gidrometizdat, 356 pp., 1967

[8] Klemp, J. B., Wilhelmson,R. B., The simulation of three-dimensional convective storm dynamics, J. Atmos. Sci., 35, 1070-1096, 1978

[9] Baldauf, M., Brdar, S., An Analytic Solution for Linear Gravity Waves in a Channel as a Test for Numerical Models using the Non-Hydrostatic, Compressible Euler Equations, Quart. J. Roy. Met. Soc. 2012 [in press]

[10] Bretherton, FP. 1966. The propagation of Groups of Internal Gravity Waves in a Shear Flow. Quart. J. Roy. Met. Soc. 92: 466-480.